

Structures of $[(\text{CO}_2)_n(\text{H}_2\text{O})_m]^-$ ($n = 1-4$, $m = 1, 2$) cluster anions. I.

Infrared photodissociation spectroscopy

Azusa Muraoka and Yoshiya Inokuchi

*Department of Basic Science, Graduate School of Arts and Sciences,
The University of Tokyo, Komaba, Meguro-ku, Tokyo 153-8902, Japan*

Nobuyuki Nishi

Institute for Molecular Science, Myodaiji, Okazaki 444-8585, Japan

Takashi Nagata^{a)}

*Department of Basic Science, Graduate School of Arts and Sciences,
The University of Tokyo, Komaba, Meguro-ku, Tokyo 153-8902, Japan*

ABSTRACT

The infrared photodissociation spectra of $[(\text{CO}_2)_n(\text{H}_2\text{O})_m]^-$ ($n = 1-4$, $m = 1, 2$) are measured in the 3000–3800 cm^{-1} range. The $[(\text{CO}_2)_n(\text{H}_2\text{O})_1]^-$ spectra are characterized by a sharp band around 3570 cm^{-1} except for $n = 1$; $[(\text{CO}_2)_1(\text{H}_2\text{O})_1]^-$ does not photodissociate in the spectral range studied. The $[(\text{CO}_2)_n(\text{H}_2\text{O})_2]^-$ ($n = 1, 2$) species have similar spectral features with a broad band at $\approx 3340 \text{ cm}^{-1}$. A drastic change in the spectral features is observed for $[(\text{CO}_2)_3(\text{H}_2\text{O})_2]^-$, where sharp bands appear at 3224, 3321, 3364, 3438, and 3572 cm^{-1} . *Ab initio* calculations are performed at the MP2/6-311++G** level to provide structural information such as optimized structures, stabilization energies, and vibrational frequencies of the $[(\text{CO}_2)_n(\text{H}_2\text{O})_m]^-$ species. Comparison between the experimental and theoretical results reveals rather size- and composition-specific hydration manner in $[(\text{CO}_2)_n(\text{H}_2\text{O})_m]^-$: (1) the incorporated H_2O is bonded to either CO_2^- or C_2O_4^- through two equivalent $\text{OH}\cdots\text{O}$ hydrogen bonds to form a ring structure in $[(\text{CO}_2)_n(\text{H}_2\text{O})_1]^-$; (2) two H_2O molecules are independently bound to the O atoms of CO_2^- in $[(\text{CO}_2)_n(\text{H}_2\text{O})_2]^-$ ($n = 1, 2$); (3) a cyclic structure composed of CO_2^- and two H_2O molecules is formed in $[(\text{CO}_2)_3(\text{H}_2\text{O})_2]^-$.

^{a)} Author to whom correspondence should be addressed.

I. INTRODUCTION

Hydration plays an important role both in the solution and gas-phase chemistry, especially when ionic species take part in the chemical processes. Among a variety of solvent effects induced by hydration, the stabilization mechanism of charged species via the formation of hydrogen-bonded structures is one of the most fundamental issues; there have been a number of investigations on this issue both experimentally and theoretically.¹⁻³ In those extensive investigations, hydrates of gas-phase atomic/molecular ions have often been exploited as appropriate systems for the microscopic understanding of the nature of hydration. Here, we propose another type of system exploitable for the investigation of hydration effects: i.e., the cluster anions of carbon dioxide including one or two H₂O molecule(s), [(CO₂)_n(H₂O)_m]⁻ ($m = 1, 2$). The formation of [(CO₂)_n(H₂O)_m]⁻ and their distinct stability against autodetachment were first reported by Klots.⁴ Recent experimental^{5, 6} and theoretical⁷ studies have further revealed that hydration plays a crucial role to localize the charge distribution in [(CO₂)_n(H₂O)_m]⁻, and that the behavior of charge localization strongly depends on the cluster size and composition. These properties characteristic of [(CO₂)_n(H₂O)_m]⁻ can be probed experimentally by negative-ion photoelectron spectroscopy. Figure 1 displays an overview of the [(CO₂)_n(H₂O)_m]⁻ ($1 \leq n \leq 4$, $0 \leq m \leq 2$) photoelectron spectra measured in our previous study.^{6, 8} The spectra are well approximated either by a Gaussian profile or by the superposition of two Gaussians. Each Gaussian component is attributed to the photodetachment from [(CO₂)_n(H₂O)_m]⁻ having a certain electronic structure; the band maximum corresponds to the vertical detachment energy (VDE) of the cluster anion. For [(CO₂)_n(H₂O)₁]⁻ with size $2 \leq n \leq 4$ and [(CO₂)₂(H₂O)₂]⁻, the photoelectron spectra are composed of two band components, indicating the coexistence of two types of isomers having different VDEs. For the rest of the clusters, each photoelectron spectrum shows a single Gaussian profile. With the aid of *ab initio* calculations,⁷ the following conclusions have been drawn from the photoelectron

spectroscopic measurement:

- (1) The electronic structures of $[(\text{CO}_2)_n(\text{H}_2\text{O})_m]^-$ are categorized into two groups by the extent of charge localization: one formulated as $\text{CO}_2^- \cdot (\text{CO}_2)_{n-1}(\text{H}_2\text{O})_m$ and the other as $\text{C}_2\text{O}_4^- \cdot (\text{CO}_2)_{n-2}(\text{H}_2\text{O})_m$. The former is referred to as “Type I” structure and the latter as “Type II” structure after Ref. 6. In Type I structure, the charge is localized on a CO_2 monomer, while C_2O_4^- is formed as the anionic core in Type II structure. These two forms of $[(\text{CO}_2)_n(\text{H}_2\text{O})_m]^-$ are designated as “electronic isomers” because they are constitutional isomers having different electronic structures. The electronic isomers have a VDE difference of ≈ 1.2 eV as observed by photoelectron spectroscopy.
- (2) The Type I and Type II isomers coexist in $[(\text{CO}_2)_n(\text{H}_2\text{O})_1]^-$ with size $2 \leq n \leq 4$ and in $[(\text{CO}_2)_2(\text{H}_2\text{O})_2]^-$, while the Type I component dominates the $[(\text{CO}_2)_n(\text{H}_2\text{O})_2]^-$ ($n = 3, 4$) spectra. These phenomena present a sharp contrast to the $(\text{CO}_2)_n^-$ case, where the $n = 2-4$ members exclusively take on Type II structure. The incorporation of H_2O into $(\text{CO}_2)_n^-$ tends to increase the relative abundance of Type I structure.

In the present study, we apply infrared photodissociation (IPD) spectroscopy to the $[(\text{CO}_2)_n(\text{H}_2\text{O})_m]^-$ system in order to obtain further information on the hydrogen-bonded structures formed in the cluster anions. The IPD method has been successfully employed by several research groups to investigate the gas-phase hydrates of small anions such as F^- , Cl^- , Br^- , I^- , Cl_2^- , NO^- , OH^- , O_2^- .⁹⁻²² Here, the IPD spectra of $[(\text{CO}_2)_n(\text{H}_2\text{O})_m]^-$ ($n = 1-4$, $m = 1, 2$) are observed in the OH stretching region ($3000-3800 \text{ cm}^{-1}$). We also extend *ab initio* calculations for $[(\text{CO}_2)_n(\text{H}_2\text{O})_m]^-$ up to $n = 3$ and $m = 2$ with higher level of approximation than that in the previous study.⁷ The calculations provide optimized geometries for $[(\text{CO}_2)_n(\text{H}_2\text{O})_m]^-$ along with their vibrational frequencies, which can be compared directly with the experimental IPD spectra. The structural properties of hydration in $[(\text{CO}_2)_n(\text{H}_2\text{O})_m]^-$ are discussed on the basis of the observed IPD spectral features in conjunction with the calculation results.

II. EXPERIMENT

The IPD spectra of $[(\text{CO}_2)_n(\text{H}_2\text{O})_m]^-$ are measured by an ion-guide spectrometer equipped with two quadrupole mass filters.²³ The negative ion source and the source condition employed in the present experiment are almost identical to those in the previous photoelectron experiment.⁶ Therefore, we assume that $[(\text{CO}_2)_n(\text{H}_2\text{O})_m]^-$ prepared in the present study have the same properties, such as size distributions, internal energies, and relative abundance of isomers, as in the previous experiment. Even though there is a small difference in the source conditions between the two experiments, the validity of the above assumption is assured by the fact that the photoelectron spectral features scarcely depend on the source conditions and the formation processes of the clusters.⁶ The target $[(\text{CO}_2)_n(\text{H}_2\text{O})_m]^-$ is prepared as follows. A gas mixture of carbon dioxide and water (a total stagnation pressure of $1\text{--}2 \times 10^5$ Pa) is introduced into the vacuum chamber through a pulsed nozzle (General Valve Series 9) with a repetition rate of 10 Hz. A homemade electron-impact ionizer is situated near the exit of the pulsed nozzle, where the pulsed free jet is crossed with a continuous electron beam to produce secondary slow electrons. The slow electrons are attached to neutral $[(\text{CO}_2)_N(\text{H}_2\text{O})_M]$ clusters to form the $[(\text{CO}_2)_n(\text{H}_2\text{O})_m]^-$ cluster anions.⁶ After passing through a skimmer, cluster ions are accelerated into the first quadrupole mass filter by a 50-eV pulsed voltage. Mass-selected ions of interest are then introduced into a quadrupole ion guide through a 90° ion bender. The ion beam is merged with an output of a pulsed infrared photodissociation laser in the ion guide. Resultant fragment ions are mass-analyzed by the second quadrupole mass filter and detected by a secondary electron multiplier tube. The IPD spectra of the parent ions are obtained by plotting the yields of fragment ions against wavenumber of the dissociation laser. The dissociation channel monitored for the IPD spectra of $[(\text{CO}_2)_n(\text{H}_2\text{O})_m]^-$ is the loss of one CO_2 molecule except for $[(\text{CO}_2)_1(\text{H}_2\text{O})_2]^-$; an H_2O molecule is ejected by the infrared irradiation of $[(\text{CO}_2)_1(\text{H}_2\text{O})_2]^-$. No other dissociation pathway can be detected in the present

experiment.

The tunable infrared source used in this study is an optical parametric oscillator system (Continuum Mirage 3000) pumped with an injection-seeded Nd:YAG laser (Continuum Powerlite 9010). The output energy is about 1–2 mJ•pulse⁻¹ with a linewidth of ≈ 1 cm⁻¹. The infrared laser is loosely focused by a CaF₂ lens ($f = 1000$ mm) located before the ion guide.

Ab initio MO calculations are carried out with the GAUSSIAN 98 program package²⁴ in order to estimate the structural and spectroscopic properties of $[(\text{CO}_2)_n(\text{H}_2\text{O})_m]^-$, such as optimized geometries, vibrational frequencies, total energies, and VDE values.²⁵ Geometry optimization and vibrational frequency analysis are made at the MP2/6-311++G** level of theory. Total energies and VDE values are evaluated by the single-point energy calculations at the CCSDT/6-311++G** level with the optimized structures obtained in the MP2/6-311++G** calculations (CCSDT/6-311++G**//MP2/6-311++G**). To compare the calculated vibrational frequencies with observed ones, a scaling factor of 0.9397 is employed for all the frequencies calculated. This factor is determined so as to reproduce the OH stretching vibrational frequencies of a free H₂O molecule. Details of the calculations will be described in a succeeding publication,²⁵ and only a part of the results are used for discussion in this paper.

III. RESULTS AND DISCUSSION

A. Infrared photodissociation spectra of $[(\text{CO}_2)_n(\text{H}_2\text{O})_m]^-$

Figure 2 presents an overview of the IPD spectra of $[(\text{CO}_2)_n(\text{H}_2\text{O})_m]^-$ ($n = 1-4$, $m = 1, 2$) measured in the 3000–3800 cm⁻¹ range. Spectral features for the $m = 1$ species differ significantly from those for $m = 2$ in terms of the band position and intensity. The $[(\text{CO}_2)_n(\text{H}_2\text{O})_1]^-$ spectra exhibit rather simple features with a sharp peak around 3600 cm⁻¹, while in the $[(\text{CO}_2)_n(\text{H}_2\text{O})_2]^-$

spectra main features appear in the 3200–3500 cm^{-1} range. The maximum intensity of the $[(\text{CO}_2)_2(\text{H}_2\text{O})_1]^-$ band is roughly estimated to be 10% of that of the $[(\text{CO}_2)_2(\text{H}_2\text{O})_2]^-$ band. We infer qualitatively from these experimental findings that $[(\text{CO}_2)_n(\text{H}_2\text{O})_1]^-$ and $[(\text{CO}_2)_n(\text{H}_2\text{O})_2]^-$ contain different types of hydrogen-bonded structures.

As shown in Fig. 2(a), $[(\text{CO}_2)_1(\text{H}_2\text{O})_1]^-$ does not photodissociate in this spectral range probably because of its large dissociation energy; *ab initio* calculations predict the energy required to dissociate $[(\text{CO}_2)_1(\text{H}_2\text{O})_1]^-$ into $\text{CO}_2^- + \text{H}_2\text{O}$ to be 0.72 eV (5808 cm^{-1})²⁵. The $[(\text{CO}_2)_n(\text{H}_2\text{O})_1]^-$ spectra with $n = 2$ and 3 show a sharp band at 3570 and 3577 cm^{-1} , respectively (Figs. 2(b) and 2(c)). Besides these prominent peaks, a couple of weaker but reproducible bands are observed in 3530–3620 cm^{-1} . Although there seems to be some spectral features in 3200–3400 cm^{-1} , they do not appear with reproducibility in repeated measurements. The $[(\text{CO}_2)_4(\text{H}_2\text{O})_1]^-$ spectrum has a sharp and asymmetric band around 3550 cm^{-1} (Fig. 2(d)); the peak position is located slightly lower than those of the $[(\text{CO}_2)_n(\text{H}_2\text{O})_1]^-$ ($n = 2, 3$) spectra.

The $[(\text{CO}_2)_1(\text{H}_2\text{O})_2]^-$ and $[(\text{CO}_2)_2(\text{H}_2\text{O})_2]^-$ species give almost the same IPD spectra. Two intense peaks are observed at 3249 and 3345 cm^{-1} for $[(\text{CO}_2)_1(\text{H}_2\text{O})_2]^-$ (Fig. 2(e)), and 3258 and 3340 cm^{-1} for $[(\text{CO}_2)_2(\text{H}_2\text{O})_2]^-$ (Fig. 2(f)). A noticeable difference between these two spectra is the appearance of tiny peaks at 3582 and 3624 cm^{-1} in the $[(\text{CO}_2)_2(\text{H}_2\text{O})_2]^-$ spectrum. The $[(\text{CO}_2)_3(\text{H}_2\text{O})_2]^-$ species fairly differs from $[(\text{CO}_2)_n(\text{H}_2\text{O})_2]^-$ with $n = 1$ and 2 in the spectral features. The most prominent peak in the $[(\text{CO}_2)_3(\text{H}_2\text{O})_2]^-$ spectrum appears at 3224 cm^{-1} and four sharp peaks emerge at 3321, 3364, 3438, and 3572 cm^{-1} (Fig. 2(g)). The $[(\text{CO}_2)_4(\text{H}_2\text{O})_2]^-$ species provides similar but more congested spectral features than $[(\text{CO}_2)_3(\text{H}_2\text{O})_2]^-$ (Fig. 2(h)). Several peaks are apparently observed in 3200–3600 cm^{-1} ; however, the relatively small amount of $[(\text{CO}_2)_4(\text{H}_2\text{O})_2]^-$ parent ions prevents us from determining the band positions with sufficient reliability. Although the similarity of spectral features suggests that $[(\text{CO}_2)_3(\text{H}_2\text{O})_2]^-$ and

$[(\text{CO}_2)_4(\text{H}_2\text{O})_2]^-$ possess a common hydrogen-bonded structure, we will not make further spectral analysis for $[(\text{CO}_2)_4(\text{H}_2\text{O})_2]^-$ in the present study.

B. Spectral assignments

B.1. $[(\text{CO}_2)_n(\text{H}_2\text{O})_1]^-$

In Fig. 3 the IPD spectrum of $[(\text{CO}_2)_2(\text{H}_2\text{O})_1]^-$ is compared with the vibrational spectra calculated for possible isomeric forms. The IPD spectrum shows a sharp band at 3570 cm^{-1} and a weaker one at 3618 cm^{-1} . Besides these sharp bands, a broader band appears around 3530 cm^{-1} . The presence of the 3530 cm^{-1} component is significant; the band envelope of the IPD spectrum turns out to be well represented by a superposition of three Lorentz functions as indicated by the dotted lines in Fig. 3. The reproducibility of these band structures was checked carefully by a set of different measurements.

The present *ab initio* calculations predict the existence of nine stable isomeric forms for $[(\text{CO}_2)_2(\text{H}_2\text{O})_1]^-$ at the MP2/6-311++G** level.²⁵ Among those nine isomeric forms, only three are shown in Figs. 3(a)–(c). They are selected as the lowest-energy representatives of the isomers having different hydrogen-bonded structures, and providing vibrational spectral patterns comparable to the IPD spectrum as well. Forms **2-1A** and **2-1B** belong to Type II structure (C_2O_4^- core), and **2-1C** to Type I structure (CO_2^- core). Here, in the notation for the isomeric forms, the first digit of “*n-mX*” represents the number *n* of CO_2 molecules involved in the cluster anion, the second digit the number *m* of H_2O molecules, and the last character “**X**” is for identifying the individual structure. While **2-1A** is the global minimum structure of $[(\text{CO}_2)_2(\text{H}_2\text{O})_1]^-$, **2-1A** – **2-1C** are all close in energy: **2-1B** and **2-1C** are located 0.074 and 0.058 eV above **2-1A**, respectively, at the CCSDT/6-311++G**//MP2/6-311++G** level. Because of the small energy differences, all the isomeric forms shown in Fig. 3 are thought of as candidates contributable to the observed IPD

spectrum. As the spectral patterns for **2-1A** and **2-1B** well resemble each other, they are indistinguishable by infrared spectroscopy. The frequencies of the OH stretching vibrations of **2-1C** are calculated to be slightly lower than those of **2-1A** and **2-1B**, probably because the charge density of CO_2^- is higher than that of C_2O_4^- and, as a result, the intermolecular interaction between the core ion and H_2O is stronger in the Type I isomers.

Considering those findings that the IPD spectrum is composed of three vibrational bands and that there exist only two types of OH oscillations, symmetric and antisymmetric, for each predicted isomer, we conclude that at least two forms of isomers make contribution to the $[(\text{CO}_2)_2(\text{H}_2\text{O})_1]^-$ spectrum. The 3570 and 3618 cm^{-1} bands are assigned respectively to the symmetric and antisymmetric OH stretching vibrations of **2-1A** and/or **2-1B**, and the weaker band around 3530 cm^{-1} to the symmetric OH stretching vibration of **2-1C**. The antisymmetric OH band of the Type I isomer is expected to occur with an intensity much weaker than the symmetric band; it does not appear explicitly due possibly to the overlap with the 3570 cm^{-1} band. The IPD spectral features of $[(\text{CO}_2)_2(\text{H}_2\text{O})_1]^-$ is thus interpreted as the superposition of the vibrational bands of isomers **2-1A–2-1C**. The prominence of the 3570 cm^{-1} band suggests that the dominant $[(\text{CO}_2)_2(\text{H}_2\text{O})_1]^-$ species take on Type II structure. This inference is in consonance with our previous finding that the Type II component dominates the photoelectron spectrum (see Fig. 1).⁶ The $[(\text{CO}_2)_2(\text{H}_2\text{O})_1]^-$ having Type II structure eventually ejects a CO_2 molecule by breaking the C–C bond of C_2O_4^- upon the infrared photodissociation. *Ab initio* calculations also predict the preferential occurrence of the CO_2 ejection in terms of the bond dissociation energies: for example, in the case of **2-1B**, the energies required to access the dissociation limits of $\text{C}_2\text{O}_4^- + \text{H}_2\text{O}$ and $\text{CO}_2^- \cdot \text{H}_2\text{O} + \text{CO}_2$ are estimated to be 0.64 and 0.27 eV (5160 and 2150 cm^{-1}), respectively.²⁵

Figure 4 exhibits the IPD spectrum of $[(\text{CO}_2)_3(\text{H}_2\text{O})_1]^-$ along with the calculated vibrational spectra. The spectral features for $[(\text{CO}_2)_3(\text{H}_2\text{O})_1]^-$ almost mimic those for $[(\text{CO}_2)_2(\text{H}_2\text{O})_1]^-$; a sharp

band at 3577 cm^{-1} , a weak one at 3620 cm^{-1} , and a small hump at 3530 cm^{-1} are observed. The close resemblance between the two spectra suggests that $[(\text{CO}_2)_3(\text{H}_2\text{O})_1]^-$ contains the **2-1A–2-1C** configurations as structural subunits. Among 15 stable isomeric forms predicted for $[(\text{CO}_2)_3(\text{H}_2\text{O})_1]^-$,²⁵ nine forms meet this structural requirement. The lowest-energy representatives of different hydrogen-bonded structures are shown as **3-1A–3-1C** in Fig. 4. Form **3-1A** is the global minimum structure; the energy difference from **3-1A** is calculated to be 0.038 eV for **3-1B**, and 0.076 eV for **3-1C** at the CCSDT/6-311++G**//MP2/6-311++G** level. On the analogy of the $[(\text{CO}_2)_2(\text{H}_2\text{O})_1]^-$ case, the 3577 and 3620 cm^{-1} bands are assigned to the symmetric and antisymmetric OH stretching vibrations of **3-1A** and/or **3-1B**. The position of the 3530 cm^{-1} band coincides fairly well with that of the symmetric OH stretching vibration of **3-1C**. As is the case in $[(\text{CO}_2)_2(\text{H}_2\text{O})_1]^-$, the $[(\text{CO}_2)_3(\text{H}_2\text{O})_1]^-$ spectrum arises from the coexistence of Type I and Type II structures. Since the most intense band is attributed to Type II structure, the major species existing in our beam possesses a C_2O_4^- core.

As for the $[(\text{CO}_2)_4(\text{H}_2\text{O})_1]^-$ species, we could not complete *ab initio* calculations due to a formidable computational time at the MP2/6-311++G** level. This prevents us from a direct comparison between observed and calculated spectra in the $n = 4$ case. The observed $[(\text{CO}_2)_4(\text{H}_2\text{O})_1]^-$ spectral profile is found to be decomposed into two components centered at 3551 and 3582 cm^{-1} . By comparing the $[(\text{CO}_2)_n(\text{H}_2\text{O})_1]^-$ spectra for $n = 2 - 4$, we tentatively assign the 3551 and 3582 cm^{-1} components to the symmetric OH stretching vibrations of Type I and Type II isomers of $[(\text{CO}_2)_4(\text{H}_2\text{O})_1]^-$, respectively. This assignment is in consonance with the photoelectron result indicating the coexistence of Type I and Type II isomers in $[(\text{CO}_2)_4(\text{H}_2\text{O})_1]^-$ (see Fig. 1).⁶

B.2. $[(\text{CO}_2)_n(\text{H}_2\text{O})_2]^-$

The IPD spectrum of $[(\text{CO}_2)_1(\text{H}_2\text{O})_2]^-$ consists of two components at 3249 and 3345 cm^{-1} as

depicted in the top panel of Fig. 5. Eight possible isomeric forms are predicted for $[(\text{CO}_2)_1(\text{H}_2\text{O})_2]^-$ at the MP2/6-311++G** level.²⁵ The global minimum structure, **1-2A**, is shown in Fig. 5(a). Form **1-2B** (Fig. 5(b)) is the lowest-energy isomer whose spectral pattern matches the IPD spectral features. The energy difference between **1-2A** and **1-2B** is calculated to be 0.068 eV at the CCSDT/6-311++G**//MP2/6-311++G** level. Although the spectral position of the strongest band of **1-2A** almost coincides with the observed value of 3345 cm^{-1} , other vibrational transitions expected for **1-2A** are not observed around 3550 cm^{-1} . The contribution of **1-2A** to the IPD spectrum is rather minor, if exist. The 3345 cm^{-1} band is eventually assigned to the almost degenerate hydrogen-bonded OH oscillations of **1-2B**. The 3249 cm^{-1} band is assignable to the overtone of the H_2O bending vibration, which borrows band intensity from the 3345 cm^{-1} transition via a resonance coupling. This assignment is based on the fact that no isomeric form predicted by *ab initio* calculations can elucidate the occurrence of the 3249 cm^{-1} transition, and that bending overtone is often observed in the IPD spectra of hydrated anion systems.¹⁰⁻²² The band positions for free OH oscillations are theoretically predicted to be $\approx 3710\text{ cm}^{-1}$ for **1-2B**; they are not detected in the present experiment due possibly to their small oscillator strengths.

As the energy required to eliminate one H_2O molecule from **1-2B** to form $[(\text{CO}_2)_1(\text{H}_2\text{O})_1]^-$ is calculated to be 0.587 eV at the CCSDT/6-311++G**//MP2/6-311++G** level, $[(\text{CO}_2)_1(\text{H}_2\text{O})_2]^-$ in the vibrational ground state should undergo single-photon dissociation only for the irradiation with $\bar{\nu} > 4735\text{ cm}^{-1}$. Multiphoton processes scarcely occur under the present experimental condition where the photon density is kept below $\approx 10\text{ mJ}\cdot\text{cm}^{-2}$ in the ion guide.²³ Therefore, the present observation of the IPD spectrum suggests that $[(\text{CO}_2)_1(\text{H}_2\text{O})_2]^-$ anions formed in the electron-impact ionized jet carry internal energy enough to dissociate upon the absorption of $3100\text{--}3800\text{ cm}^{-1}$ single photon.

The resemblance between the $[(\text{CO}_2)_1(\text{H}_2\text{O})_2]^-$ and $[(\text{CO}_2)_2(\text{H}_2\text{O})_2]^-$ spectra allows us to infer

that $[(\text{CO}_2)_2(\text{H}_2\text{O})_2]^-$ species responsible for the main features of the IPD spectrum contain the **1-2B** configuration as a substructure. The MP2/6-311++G** calculations provide 20 possible isomeric forms for $[(\text{CO}_2)_2(\text{H}_2\text{O})_2]^-$; 16 isomers out of them have Type I structure and the rest four have Type II structure.²⁵ The global minimum structure, **2-2A**, is of Type II as shown in Fig. 6(a). One of the Type I isomers, **2-2B**, is 0.062 eV higher in energy. From the comparison between observed and calculated spectra, we conclude that the 3340 cm^{-1} band arises primarily from the hydrogen-bonded OH oscillations of **2-2B** (Fig. 6(b)). As is the case in $[(\text{CO}_2)_1(\text{H}_2\text{O})_2]^-$, the 3258 cm^{-1} band is ascribed to the overtone of the H_2O bending vibration. The ratio of band intensities for the 3258 and 3340 cm^{-1} transitions stands at $\approx 0.1:1$ with the band separation of 82 cm^{-1} , whereas the corresponding quantities are $\approx 0.3:1$ and 96 cm^{-1} in $[(\text{CO}_2)_1(\text{H}_2\text{O})_2]^-$. This suggests that the resonance coupling between the H_2O bend overtone and the hydrogen-bonded OH stretch is weaker in the **2-2B** configuration than in **1-2B**.

A key to the assignment of the 3582 and 3624 cm^{-1} bands is given by the previous results of photoelectron spectroscopy: Type I and Type II isomers are found to coexist in $[(\text{CO}_2)_2(\text{H}_2\text{O})_2]^-$ (see Fig. 1). As *ab initio* calculations provide Type II isomer **2-2A** as the global minimum structure, we ascribe the 3582 and 3624 cm^{-1} bands to **2-2A**. This assignment is consistent well with the $[(\text{CO}_2)_n(\text{H}_2\text{O})_1]^-$ ($n = 2, 3$) results: the band positions ($\approx 3600 \text{ cm}^{-1}$) and separation ($\approx 40 \text{ cm}^{-1}$) are almost identical with those ascribed to the Type II isomers of $[(\text{CO}_2)_n(\text{H}_2\text{O})_1]^-$ ($n = 2, 3$) (see Figs. 3 and 4). *Ab initio* calculations also suggest that the dissociation channel, **2-2A** \rightarrow **1-2B** + CO_2 , is energetically accessible: the dissociation energy is calculated to be 0.41 eV (3346 cm^{-1}).²⁵

Finally we are left with $[(\text{CO}_2)_3(\text{H}_2\text{O})_2]^-$. As readily seen in Fig. 7, the IPD spectrum of $[(\text{CO}_2)_3(\text{H}_2\text{O})_2]^-$ displays congested features quite different from those of the smaller clusters, $[(\text{CO}_2)_n(\text{H}_2\text{O})_2]^-$ with $n = 1$ and 2, possibly because the number of coexisting isomers increases with the cluster size and/or because the hydration manner changes drastically in $[(\text{CO}_2)_3(\text{H}_2\text{O})_2]^-$. In our

ab initio calculations, 26 stable geometries are found for $[(\text{CO}_2)_3(\text{H}_2\text{O})_2]^-$.²⁵ The global minimum structure, shown as **3-2A** in Fig. 7(a), possesses a CO_2^- core, being consistent with the predominance of Type I component in the photoelectron spectrum (Fig. 1). The vibrational spectral pattern calculated for **3-2A** agrees with the experimental IPD spectrum: the 3438 and 3572 cm^{-1} bands are assignable to the OH stretching vibrations predicted at 3496 and 3584 cm^{-1} , respectively. The 3224 and 3321 cm^{-1} bands arise from the coupling between the hydrogen-bonded OH vibration and the overtone of the H_2O bending vibration. A weak band at 3364 cm^{-1} is tentatively assigned to a combination band. The enhanced intensity of the 3224 cm^{-1} band is attributed possibly to the increase in the coupling between the hydrogen-bonded OH stretch and the H_2O bend overtone, and/or to accidental overlap with the vibrational bands of other low-lying isomers. In Fig. 7(b) shown is one of the low-lying isomers, **3-2B**, located 0.02 eV above **3-2A**. In isomer **3-2B**, the OH stretch decreases in energy down to $\approx 3250 \text{ cm}^{-1}$, being quite close to –or even lower than– the H_2O bend overtone ($\approx 1630 \text{ cm}^{-1}$).²⁵ Coexistence of those low-lying isomers gives rise to the complexity and anomaly in the $[(\text{CO}_2)_3(\text{H}_2\text{O})_2]^-$ spectral features.

C. Structural motif in $[(\text{CO}_2)_n(\text{H}_2\text{O})_m]^-$

On the basis of the discussions made above, it can be inferred that (1) hydration in $[(\text{CO}_2)_n(\text{H}_2\text{O})_m]^-$ ($m = 1-4$, $n = 1, 2$) occurs with H_2O molecules interacting directly with either CO_2^- or C_2O_4^- core via $\text{OH}\cdots\text{O}$ hydrogen bonds, and that (2) the hydrated anion-core in each $[(\text{CO}_2)_n(\text{H}_2\text{O})_m]^-$ forms a structural “motif” responsible for the infrared photoabsorption in the 3000–3800 cm^{-1} range. Properties of the structural motifs existing in the $[(\text{CO}_2)_m(\text{H}_2\text{O})_n]^-$ species are summarized in Fig. 8. In $[(\text{CO}_2)_n(\text{H}_2\text{O})_1]^-$ with $n = 2$ and 3, the predominant structural motif is such that H_2O bridges two oxygen atoms of C_2O_4^- , whereas in the larger cluster, $[(\text{CO}_2)_4(\text{H}_2\text{O})_1]^-$, a ring structure composed of CO_2^- and H_2O emerges as the structural motif. In these motifs

containing one H₂O molecule, vibrational modes in the 3000–3800 cm⁻¹ range arise mainly from the symmetric and antisymmetric OH stretching vibrations localized in the H₂O moiety. The vibrational frequencies tend to be lower in the Type I motif (CO₂⁻•H₂O) than in the Type II motifs (C₂O₄⁻•H₂O), due probably to the increase in the hydrogen-bond strength in the Type I motif. This comes from the higher concentration of the excess charge on CO₂⁻: the Mulliken charge populations are calculated to be -0.54 on the O atoms of CO₂⁻, whereas ≈-0.40 on the hydrogen-bonded O atoms of C₂O₄⁻.²⁵

It is interesting to compare the present findings with those reported by Johnson and coworkers on a series of monohydrated molecular anions having a double ionic hydrogen-bonding (DIHB) configuration, such as CS₂⁻•H₂O, OCS⁻•H₂O, SO₂⁻•H₂O, CH₃NO₂⁻•H₂O, and CH₃CO₂⁻•H₂O.^{26, 27} They have found that the monohydrates of CS₂⁻, OCS⁻, and SO₂⁻ provide simple OH stretching spectra characteristic of the DIHB configuration whereas the CH₃NO₂⁻•H₂O and CH₃CO₂⁻•H₂O spectra display a progression of closely spaced bands in the OH stretching region. This progression arises from strong anharmonic coupling between the hydrogen-bonded OH stretch and intermolecular rock vibration.²⁷ From the similarity observed in the IPD spectral features, we infer that [(CO₂)_n(H₂O)₁]⁻ belongs to the same category as CS₂⁻•H₂O, OCS⁻•H₂O, SO₂⁻•H₂O in terms of the hydration manner.

An introduction of another H₂O into the cluster system changes the motif drastically: two H₂O molecules are independently bonded to the O atoms of the CO₂⁻ core in [(CO₂)₁(H₂O)₂]⁻. In this motif, vibrational motions occur in a complicated but concerted manner: two vibrational modes with lower frequencies arise primarily from combinations of the stretching modes of the hydrogen-bonded OH groups, while those with higher frequencies are composed of the stretching vibrations of the free OH groups. The same structural motif remains also in [(CO₂)₂(H₂O)₂]⁻ while Type II isomer coexists in this species. In [(CO₂)₃(H₂O)₂]⁻, the structural motif is an eight-membered ring

consisting of CO_2^- and two H_2O molecules. Thus, $[(\text{CO}_2)_m(\text{H}_2\text{O})_n]^-$ ($m = 1-4$, $n = 1, 2$) exhibit rather size- and composition-specific hydration manner.

IV. CONCLUSION

We have observed the infrared photodissociation (IPD) spectra of binary cluster anions of carbon dioxide and water, $[(\text{CO}_2)_n(\text{H}_2\text{O})_m]^-$ ($n = 1-4$, $m = 1, 2$). The IPD spectra for the $m = 1$ species are characterized by a sharp vibrational band around 3600 cm^{-1} , whereas those for the $m = 2$ species by intense photoabsorption bands around 3400 cm^{-1} . *Ab initio* MO calculations have been carried out in order to obtain the optimized structures, vibrational frequencies, total energies, and VDEs of $[(\text{CO}_2)_n(\text{H}_2\text{O})_m]^-$. The spectral analyses with the aid of *ab initio* calculations reveal that all the water molecules in the clusters are directly bonded to the CO_2^- or C_2O_4^- core forming structural motifs, which primarily govern the IPD spectral features. It is also revealed that the structural motif is identical in the $n = 2-4$, $m = 1$ species whereas the motif appearing in the $n = 1-2$, $m = 2$ does not play the leading role in the $n = 3$, $m = 2$ species. The present findings possibly indicate a complex formation mechanism of $[(\text{CO}_2)_m(\text{H}_2\text{O})_n]^-$ involving $(\text{CO}_2)_M \bullet (\text{H}_2\text{O})_N + e^-$ collisions followed by electron capture, ion-core formation, solvent migration, and evaporative cooling.

ACKNOWLEDGMENTS

We are grateful to Professor K. Takatsuka for the loan of high-performance computers (HIT PSC-P4L). We are also indebted to Drs. H. Ushiyama and Y. Arasaki for their technical help in the computational study. Part of the *ab initio* calculations is performed by using the computer

systems (NEC SX-7 and Fujitsu VPP5000) at Research Center for Computational Science (RCCS), Okazaki Research Facilities, National Institutes of Natural Sciences (NINS). This work is supported by Grant-in-Aids (Grant Nos. 15350006 and 16750016) for Scientific Research from the Ministry of Education, Culture, Sports, Science and Technology (MEXT).

REFERENCES

- ¹ P. Kebarle, *Ann. Rev. Phys. Chem.* **28**, 455 (1977).
- ² R. G. Keesee and A. W. Castleman, Jr., in *Ion and Cluster Ion Spectroscopy and Structure*, edited by J. P. Maier (Elsevier, New York, 1989).
- ³ *Clusters of Atoms and Molecules II*, edited by H. Haberland (Springer-Verlag, Berlin, 1994).
- ⁴ C. E. Klots, *J. Chem. Phys.* **71**, 4172 (1979).
- ⁵ T. Nagata, H. Yoshida, and T. Kondow, *Chem. Phys. Lett.* **199**, 205 (1992).
- ⁶ T. Tsukuda, M. Saeki, R. Kimura, and T. Nagata, *J. Chem. Phys.* **110**, 7846 (1999).
- ⁷ M. Saeki, T. Tsukuda, S. Iwata, and T. Nagata, *J. Chem. Phys.* **111**, 6333 (1999).
- ⁸ K. H. Bowen and J. G. Eaton, in *The Structure of Small Molecules and Ions*, edited by R. Naaman and Z. Vagar (Plenum Press, New York, 1987), p. 147.
- ⁹ J.-H. Choi, K. Kuwata, Y.-B. Cao, and M. Okumura, *J. Phys. Chem. A* **102**, 503 (2004).
- ¹⁰ O. M. Cabarcos, C. J. Weinheimer, and J. M. Lisy, *J. Chem. Phys.* **110**, 5 (1999).
- ¹¹ E. A. Price, N. I. Hammer, and M. A. Johnson, *J. Phys. Chem. A* **108**, 3910 (2004).
- ¹² E. G. Diken, J. W. Shin, E. A. Price, and M. A. Johnson, *Chem. Phys. Lett.* **387**, 17 (2004).
- ¹³ W. H. Robertson, G. H. Weddle, and M. A. Johnson, *J. Phys. Chem. A* **107**, 9312 (2003).
- ¹⁴ E. M. Myshakin, K. D. Jordan, W. H. Robertson, G. H. Weddle, and M. A. Johnson, *J. Chem. Phys.* **118**, 4945 (2003).
- ¹⁵ W. H. Robertson, E. G. Diken, E. A. Price, J. W. Shin, and M. A. Johnson, *Science* **299**, 1367 (2003).
- ¹⁶ S. A. Corcelli, J. A. Kelley, J. C. Tully, and M. A. Johnson, *J. Phys. Chem. A* **106**, 4872 (2002).
- ¹⁷ J. M. Weber, J. A. Kelley, W. H. Robertson, and M. A. Johnson, *J. Chem. Phys.* **114**, 2698 (2001).
- ¹⁸ J. A. Kelley, J. M. Weber, K. M. Lisle, W. H. Robertson, P. Ayotte, and M. A. Johnson, *Chem. Phys. Lett.* **327**, 1 (2000).

- ¹⁹ J. M. Weber, J. A. Kelley, S. B. Nielsen, P. Ayotte, and M. A. Johnson, *Science* **287**, 2461 (2000).
- ²⁰ P. Ayotte, S. B. Nielsen, G. H. Weddle, M. A. Johnson, and S. S. Xantheas, *J. Phys. Chem. A* **103**, 10665 (1999).
- ²¹ P. Ayotte, G. H. Weddle, J. Kim, and M. A. Johnson, *J. Am. Chem. Soc.* **120**, 12361 (1998).
- ²² P. Ayotte, G. H. Weddle, J. Kim, and M. A. Johnson, *Chem. Phys.* **239**, 485 (1998).
- ²³ Y. Inokuchi and N. Nishi, *J. Chem. Phys.* **114**, 7059 (2001).
- ²⁴ Gaussian 98, Revision A.11.4, M. J. Frisch, G. W. Trucks, H. B. Schlegel, G. E. Scuseria, M. A. Robb, J. R. Cheeseman, V. G. Zakrzewski, J. A. Montgomery, Jr., R. E. Stratmann, J. C. Burant, S. Dapprich, J. M. Millam, A. D. Daniels, K. N. Kudin, M. C. Strain, O. Farkas, J. Tomasi, V. Barone, M. Cossi, R. Cammi, B. Mennucci, C. Pomelli, C. Adamo, S. Clifford, J. Ochterski, G. A. Petersson, P. Y. Ayala, Q. Cui, K. Morokuma, N. Rega, P. Salvador, J. J. Dannenberg, D. K. Malick, A. D. Rabuck, K. Raghavachari, J. B. Foresman, J. Cioslowski, J. V. Ortiz, A. G. Baboul, B. B. Stefanov, G. Liu, A. Liashenko, P. Piskorz, I. Komaromi, R. Gomperts, R. L. Martin, D. J. Fox, T. Keith, M. A. Al-Laham, C. Y. Peng, A. Nanayakkara, M. Challacombe, P. M. W. Gill, B. Johnson, W. Chen, M. W. Wong, J. L. Andres, C. Gonzalez, M. Head-Gordon, E. S. Replogle, and J. A. Pople (Gaussian, Inc., Pittsburgh PA, 2002).
- ²⁵ A. Muraoka, Y. Inokuchi, and T. Nagata, *J. Chem. Phys.* to be submitted.
- ²⁶ W. H. Robertson, E. A. Price, J. M. Weber, J.-W. Shin, G. H. Weddle, and M. A. Johnson, *J. Phys. Chem. A* **107**, 6527 (2003).
- ²⁷ E. M. Myshakin, K. D. Jordan, E. L. Sibert III, and M. A. Johnson, *J. Chem. Phys.* **119**, 10138 (2003).

FIGURE CAPTIONS

Figure 1. Photoelectron spectra of $[(\text{CO}_2)_n(\text{H}_2\text{O})_m]^-$ at a photon energy of 4.66 eV. The CO_2^- spectrum is taken from Ref. 8 and the rest from Ref. 6. The numbers n - m in the figure denote the composition of $[(\text{CO}_2)_n(\text{H}_2\text{O})_m]^-$. The dots represent the experimental data. The solid curves are the best-fit Gaussian profiles (see Ref. 6). The shaded areas correspond to the band components attributed to the Type II isomers.

Figure 2. Overview of the infrared photodissociation spectra of $[(\text{CO}_2)_n(\text{H}_2\text{O})_m]^-$ measured in the 3000–3800 cm^{-1} range. The numbers n - m in the figure denote the composition of $[(\text{CO}_2)_n(\text{H}_2\text{O})_m]^-$. Note that the ordinate for the $n = 1$ spectra is expanded by a factor of ten as compared with that for the $n = 2$ spectra.

Figure 3. Infrared photodissociation spectrum of $[(\text{CO}_2)_2(\text{H}_2\text{O})_1]^-$ (top panel). The solid line represents the experimental data. Dotted lines are the band components used to reproduce the spectrum. (a)–(c) Optimized $[(\text{CO}_2)_2(\text{H}_2\text{O})_1]^-$ structures along with the corresponding vibrational spectra calculated at the MP2/6-311++G** level. One unit in the ordinate corresponds to the IR intensity of 500 $\text{km}\cdot\text{mol}^{-1}$.

Figure 4. Infrared photodissociation spectrum of $[(\text{CO}_2)_3(\text{H}_2\text{O})_1]^-$ (top panel). (a)–(c) Optimized $[(\text{CO}_2)_3(\text{H}_2\text{O})_1]^-$ structures along with the calculated vibrational spectra. One unit in the ordinate corresponds to the IR intensity of 500 $\text{km}\cdot\text{mol}^{-1}$.

Figure 5. Infrared photodissociation spectrum of $[(\text{CO}_2)_1(\text{H}_2\text{O})_2]^-$ (top panel). (a), (b) Optimized

$[(\text{CO}_2)_1(\text{H}_2\text{O})_2]^-$ structures along with the calculated vibrational spectra. One unit in the ordinate corresponds to the IR intensity of $1000 \text{ km}\cdot\text{mol}^{-1}$.

Figure 6. Infrared photodissociation spectrum of $[(\text{CO}_2)_2(\text{H}_2\text{O})_2]^-$ (top panel). (a), (b) Optimized $[(\text{CO}_2)_2(\text{H}_2\text{O})_2]^-$ structures along with the calculated vibrational spectra. One unit in the ordinate corresponds to the IR intensity of $1000 \text{ km}\cdot\text{mol}^{-1}$.

Figure 7. Infrared photodissociation spectrum of $[(\text{CO}_2)_3(\text{H}_2\text{O})_2]^-$ (top panel). (a), (b) Optimized $[(\text{CO}_2)_3(\text{H}_2\text{O})_2]^-$ structures along with the calculated vibrational spectra. One unit in the ordinate corresponds to the IR intensity of $1000 \text{ km}\cdot\text{mol}^{-1}$.

Figure 8. Properties of the structural motifs existing in the $[(\text{CO}_2)_n(\text{H}_2\text{O})_m]^-$ species. The vibrational motions and their frequencies are those predicted for the isolated structural motifs at the MP2/6-311++G** level. The motions and frequencies are modified to some extent in $[(\text{CO}_2)_n(\text{H}_2\text{O})_m]^-$, where the motifs are surrounded by solvent CO_2 molecules. The nomenclature " n - m " represents the $[(\text{CO}_2)_n(\text{H}_2\text{O})_m]^-$ species where the structure motif is formed.

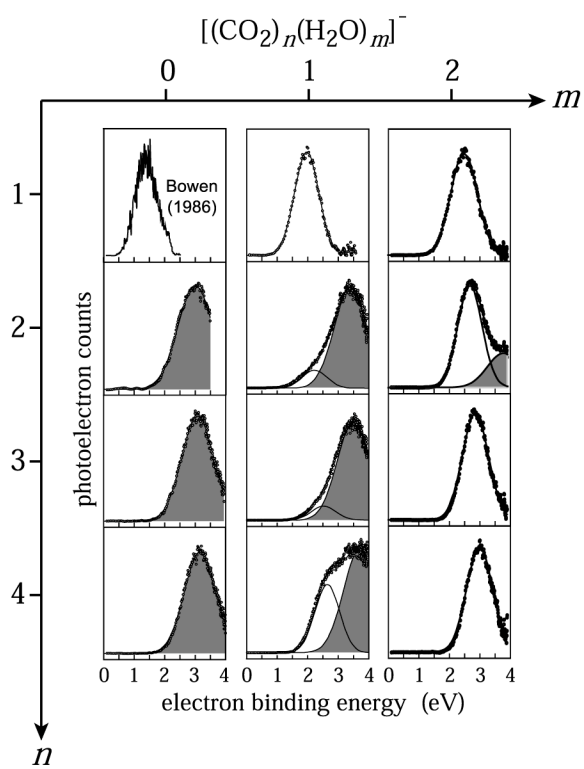


Figure 1. Muraoka et al.

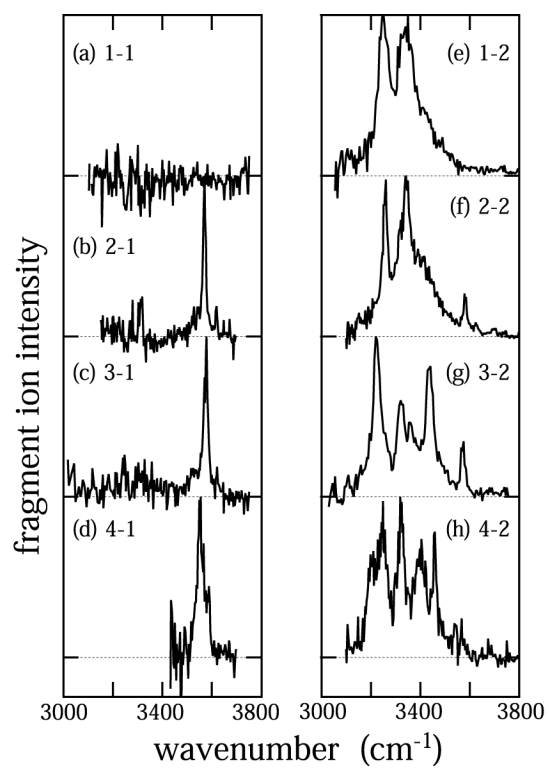


Figure 2. Muraoka et al.

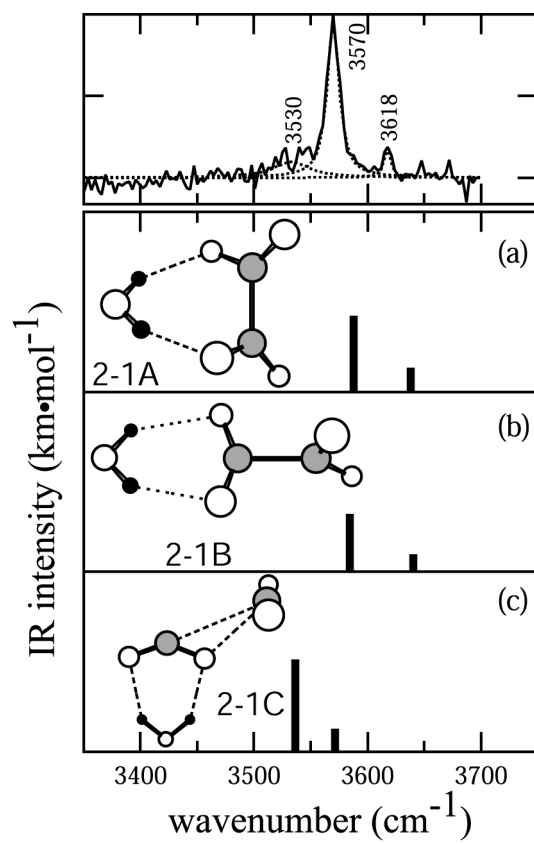


Figure 3. Muraoka et al.

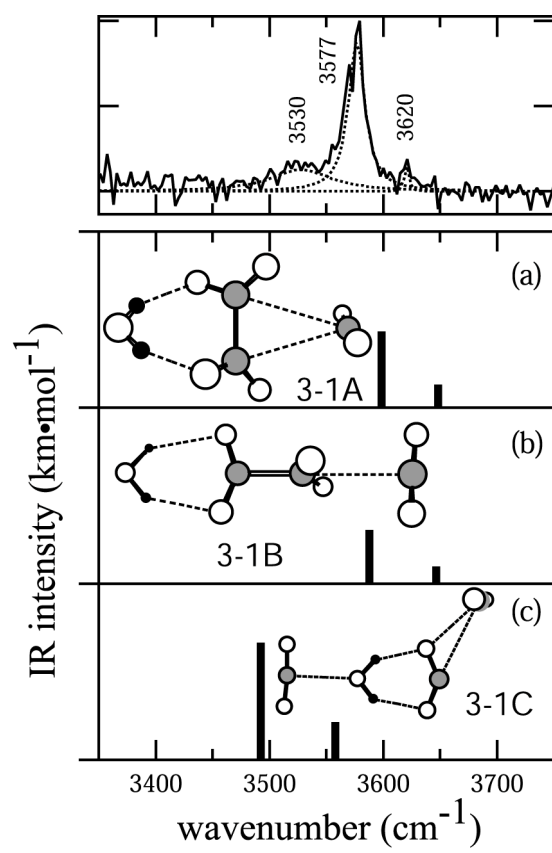


Figure 4. Muraoka et al.

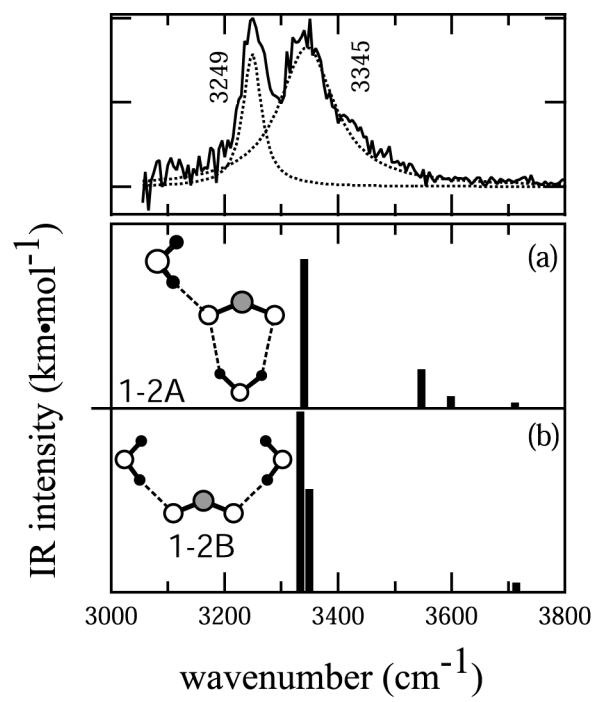


Figure 5. Muraoka et al.

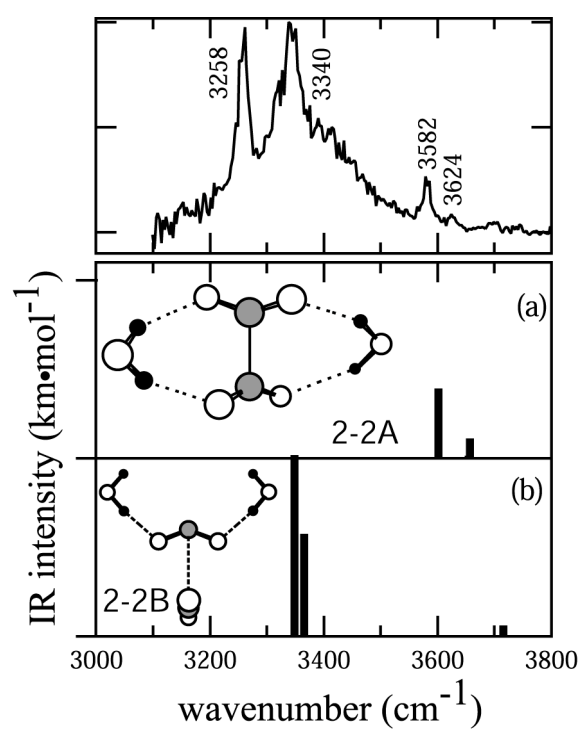


Figure 6. Muraoka et al.

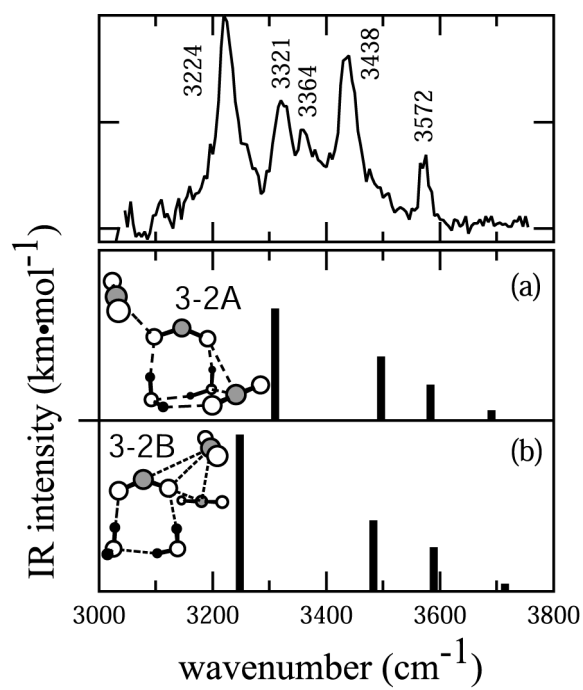


Figure 7. Muraoka et al.

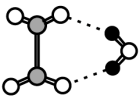
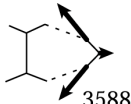
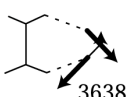

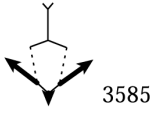
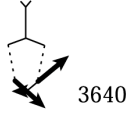
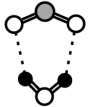
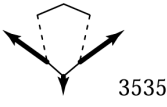

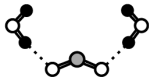

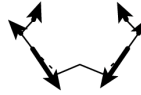

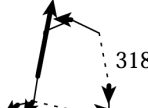
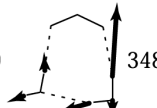
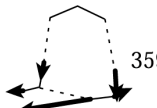
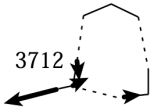
Motifs	Vibrational Modes		$n-m$
	 3588	 3638	2-1 3-1 2-2
	 3585	 3640	
	 3535	 3563	2-1 3-1 4-1
	 3333	 3349	1-2 2-2
	 3189	 3488	3-2
	 3594	 3712	

Figure 8. Muraoka et al.